Article

Not peer-reviewed version

Machine Learning-Based Estimation of Daily Reference Evapotranspiration in Vojvodina, Serbia

Milica Stajić , Dejan Mirčetić * , Atila Bezdan , Radovan Savić , Sanja Antić , Nikola Santrač , Andrea Salvai , Milena Lakićević , Boško Blagojević

Posted Date: 30 March 2026

doi: 10.20944/preprints202603.2372.v1

Keywords: reference evapotranspiration; FAO-56 Penman-Monteith; artificial neural networks; machine learning; meteorological data

 doi:10.20944/preprints202603.2372.v1

Article

Machine Learning-Based Estimation of Daily Reference Evapotranspiration in Vojvodina, Serbia

Milica Stajić [1], Dejan Mirčetić [2,*], Atila Bezdan [1], Radovan Savić [1], Sanja Antić [1], Nikola Santrač [1], Andrea Salvai [1], Milena Lakićević [1] and Boško Blagojević [1]

[1] Faculty of Agriculture, University of Novi Sad, Trg D. Obradovica 8, 21000 Novi Sad, Serbia

[2] The Institute for Artificial Intelligence of Serbia, Fruskogorska 1, Novi Sad 21000, Serbia

* Correspondence: dejan.mircetic@ivi.ac.rs

Abstract

Reference evapotranspiration (ET_0) is most commonly estimated using the FAO-56 Penman-Monteith (PM) equation. However, its application is often limited by the lack of required meteorological parameters. Due to their flexibility, ability to operate with limited input, and high accuracy in estimating ET_0, machine learning models have become increasingly relevant in scientific research, offering a practical alternative under limited data conditions. In this study, artificial neural networks (ANNs) were applied to estimate daily ET_0 using meteorological data from the Novi Sad station in Vojvodina (Serbia). The dataset consisted of eight meteorological variables relevant to evapotranspiration processes. Analysis showed that some variables had a stronger influence on ET_0 prediction than others. To evaluate their combined effect, a series of ANN models with different input combinations were developed and tested. The FAO-56 PM method was used as a benchmark, and model performance was evaluated using R2, NSE, RMSE, and MAE. The highest accuracy was achieved when all variables were included, providing the model with maximum information. The best performance was obtained using a two-hidden-layer architecture with 32 and 16 neurons, resulting in $R^2 = 0.98$, NSE = 97.86%, RMSE = 0.25 mm day^{-1}, and MAE = 0.17 mm day^{-1}.

Keywords: reference evapotranspiration; FAO-56 Penman-Monteith; artificial neural networks; machine learning; meteorological data

1. Introduction

Evapotranspiration (ET) is a key component of the hydrologic cycle, as it governs the transfer of moisture to the atmosphere and affects vital features of terrestrial ecosystems, such as runoff, soil moisture, and plant growth, which are critical to water availability [1–5]. ET is a complex process because it depends on the interactions among atmospheric, soil, and plant parameters [6]. Due to this complexity, it is essential in various fields of research, including the optimization of water resource use, crop yield simulation, irrigation and management system design, hydrological balance assessment, and improving water use efficiency in agriculture [7–9]. Accurate ET estimation is crucial for efficient irrigation management [10]. Reference evapotranspiration (ET_0) is a climatic parameter that represents the atmospheric demand for evaporation from a reference surface. The reference surface is a hypothetical grass crop with a height of 0.12 m, a fixed surface resistance of 70 s m^{-1}, and an albedo of 0.23 [11]. Accurate estimation of ET_0 is essential for simulating the global water cycle and for making irrigation decisions [12–16]. ET_0 can be determined through direct measurements, such as the use of lysimeters, which are accurate but demanding in terms of time, cost, and resources. Therefore, empirical methods are most commonly used in practice, with the FAO-56 Penman-Monteith (FAO-56 PM) equation being considered the most reliable.

According to the Food and Agriculture Organization of the United Nations (FAO), the standard method for calculating ET_0 is the FAO-56 PM equation, which has proven to be the most reliable under different climatic conditions [17–20]. The method represents a parameterized adaptation of the

 doi:10.20944/preprints202603.2372.v1

original Penman-Monteith model [21], which is a widely used physical model for estimating actual evapotranspiration. However, to calculate ET_0 using the FAO-56 PM method, numerous meteorological parameters are required, which limits its application in regions lacking complete input data [22–26]. In addition to the FAO-56 PM method, alternative approaches have been considered for calculating ET_0 in situations with a limited number of input parameters. One approach is the replacement of the FAO-56 PM equation with a simplified empirical formula, while another is the use of machine learning techniques to directly simulate ET_0 based on a reduced input set, which is the main focus of this study.

Machine learning (ML) is a technique within the field of artificial intelligence that relies on the idea that systems can learn from data, identify patterns, and make decisions with minimal human involvement [27]. ML techniques are applied in situations involving large datasets and numerous variables that change over time, particularly in domains where the use of predefined formulas or equations is difficult. ML models can be applied to predict daily ET based on extensive climatic datasets, even in the absence of detailed knowledge about the physical ET process. The application of ML techniques, particularly artificial neural networks, in modeling hydrological processes such as ET has attracted significant attention from researchers [28–35].

Artificial neural networks (ANNs) are algorithmic structures inspired by the functioning of the biological nervous system in the human brain [36,37]. ANN is frequently used for modeling ET due to its ability to recognize and reproduce complex input-output relationships without the need for detailed knowledge of the physical process [6]. Due to their flexible nature, neural networks enable the development of models without requiring prior knowledge of data distribution or interactions among variables, which is often necessary in parametric statistical methods [38].

Mallikarjuna et al. [39] investigated the applicability of linear regression and ANN models for estimating ET_0. They identified air temperature, wind speed, relative humidity, and sunshine hours as the most influential climatic variables. The optimal ANN models consistently demonstrated better performance than regression models in estimating daily ET_0. Dimitriadou and Nikolakopoulos [40] examined the use of ANN for estimating ET_0 during winter and summer months. Their study aimed to evaluate whether a reduced number of input parameters could yield satisfactory ET_0 predictions. Makwana et al. [41] examined the effectiveness of ANN in estimating ET_0 using a limited number of meteorological input parameters. Their results showed that ANN models trained with all five input variables (maximum and minimum temperature, relative humidity, wind speed, and bright sunshine hours) achieved high accuracy, while variations in input combinations and network architecture significantly affected model performance. Naresh et al. [42] evaluated the performance of ANN models for estimating ET_0 using long-term meteorological data. Their results showed that the best performance was achieved with a single hidden layer of thirteen neurons trained using the Levenberg-Marquardt algorithm. El-Magd et al. [43] developed and tested seven ANN models using different combinations of five meteorological input parameters (maximum and minimum air temperature, dew point temperature, wind speed, and precipitation) to evaluate the accuracy of the ANN in estimating ET_0. The results indicated that ANN models provided accurate estimations, particularly when the temperature-related inputs were included, while precipitation had the least influence on prediction performance. Makwana et al. [44] evaluated the performance of several AI models, including ANN, Extreme Learning Machine (ELM), M5 Tree, and Multiple Linear Regression (MLR), for estimating ET_0. The results showed that ANN models outperformed ELM, M5 Tree, and MLR in terms of various performance indicators when compared to the FAO-56 PM equation. Kumar et al. [45] used ANN models to simulate ET_0 at three meteorological stations. Different combinations of input parameters were tested and compared against the FAO-56 PM method. The best performance was achieved when all input parameters were included, while the lowest accuracy was observed when only air temperature and relative humidity were used. Skhiri et al. [46] estimated monthly ET_0 using ANN models based on meteorological data from multiple stations in Tunisia. Their study identified maximum air temperature as the most significant meteorological parameter influencing model accuracy.

 doi:10.20944/preprints202603.2372.v1

Based on previous research, this study aims to evaluate the effectiveness of ANN models in estimating ET_0 under conditions of limited availability of meteorological data, through comparison with the standard FAO-56 PM method.

2. Materials and Methods

2.1. Study Area and Data Used

The Novi Sad meteorological station, located in the region of Vojvodina (Serbia), was selected in this study for ET_0 modeling using a limited set of meteorological parameters. The study area is located at latitude 45.33°N and longitude 19.85°E, with an elevation of 84 m above mean sea level (Figure 1). Based on its geographical location, the region is classified as having a temperate continental climate. Vojvodina is characterized by an extensive network of natural watercourses and canals that are part of the Danube-Tisa-Danube hydrosystem. The region is predominantly agricultural, with more than 17,500 km^2 of arable land, representing approximately 75% of its total area. In this study, daily meteorological data were used, including maximum, minimum, and mean air temperature (T_{max}, T_{min}, T_{mean}), relative humidity (RH), wind speed (WS), global radiation (GR), precipitation (P), and mean sea level pressure (SLP), covering the period from 1950 to June 2023. The data were obtained from the Copernicus Climate Change Service (C3S) [47].

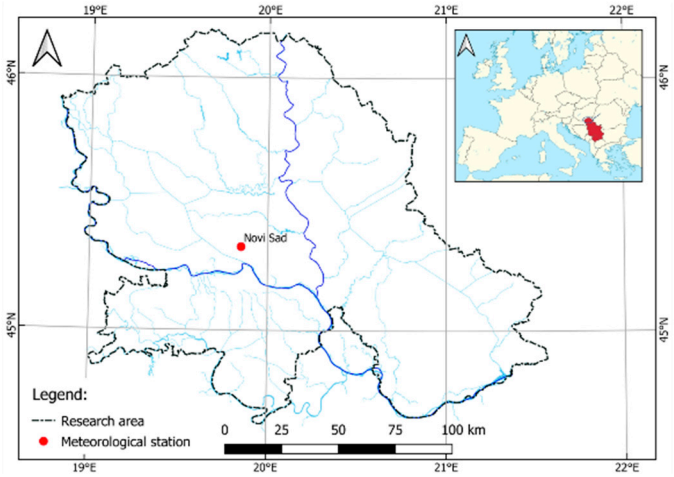

Figure 1. Location of the meteorological station used in the study.

Maximum, minimum, and mean air temperature, relative humidity, wind speed, global radiation, precipitation, and mean sea level pressure ranged from -16.3°C to 41.2°C, -29.9°C to 25.1°C, -22.4°C to 32.7°C, 21.0% to 94.0%, 0.5 to 7.3 m s^{-1}, 0.1 W m^{-2} to 470 W m^{-2}, 0 mm to 72.4 mm, and 976.6 hPa to 1046.2 hPa, respectively (Table 1). Mean values of the meteorological variables at the Novi Sad station for the period from 1950 to June 2023 are presented in Figure 2.

Table 1. Descriptive statistics of the available meteorological variables at the Novi Sad station.

Parameters	T_{max} (°C)	T_{min} (°C)	T_{mean} (°C)	RH (%)	WS (m s^{-1})	GR (W m^{-2})	P(mm)	SLP (hPa)
X_{min}	-16.3	-29.9	-22.4	21.0	0.5	0.1	0	976.6
X_{max}	41.2	25.1	32.7	94.0	7.3	470.0	72.4	1046.2
X_{mean}	16.8	6.4	11.4	74.4	2.3	152.6	1.6	1016.7
S_X	10.2	7.8	8.8	11.7	0.8	93.3	4.0	7.6

 doi:10.20944/preprints202603.2372.v1

C_V	0.6	1.2	0.8	0.2	0.3	0.6	2.5	0.1
C_{SX}	-0.3	-0.4	-0.2	-0.5	1.0	0.3	4.7	0.2

X_{min} = minimum value, X_{max} = maximum value, X_{mean} = mean value, S_X = standard deviation, C_V = coefficient of variation, C_{SX} = skewness coefficient.

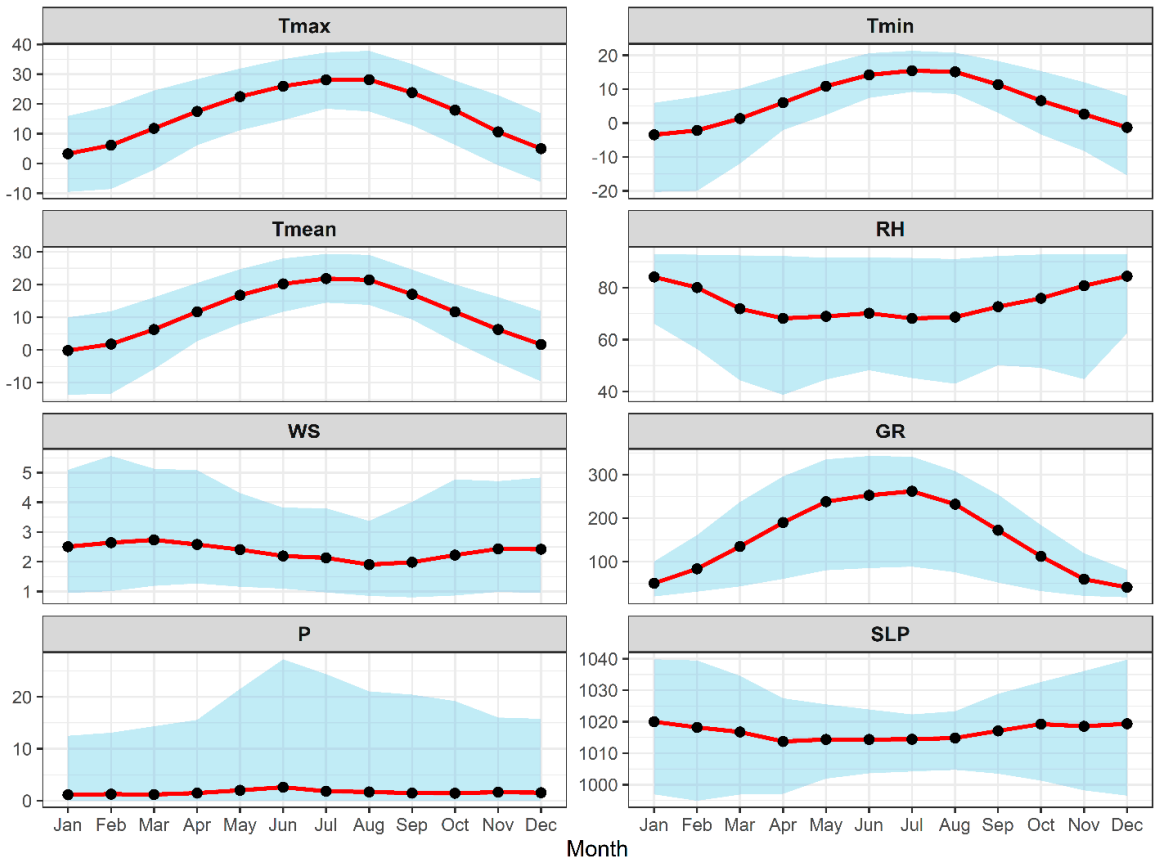

Figure 2. Mean values of the meteorological variables at the Novi Sad station for the period from 1950 to June 2023.

Mean values of the meteorological variables, as presented in Figure 2, exhibit a pronounced seasonal pattern typical for the observed region, with certain deviations. Tmax, Tmin, Tmean, and GR reach their peak during the summer months, while RH shows an inverse trend, increasing the potential for high ET_0. WS reaches its maximum in March and April and then declines during the summer period, whereas P records a peak in May and June, followed by a decrease in July and August, posing a risk of water deficit during the phase of highest crop water demand. By contrast, SLP displays an atypical seasonal pattern, with a maximum in January and a minimum in April, deviating from expected trends and indicating regional specificities in air mass circulation.

Figure 3 illustrates the seasonal evolution of eight meteorological variables: T_{max}, T_{min}, T_{mean}, RH, WS, GR, P, and SLP. Each facet corresponds to one variable, and the width of the ridges represents the density of daily values for each month. The y-axis shows months from January (top) to December (bottom), highlighting seasonal patterns. For example, temperature variables (T_{max}, T_{min}, T_{mean}) show clear peaks in summer months and minima in winter, while P and RH exhibit distinct seasonal variability. WS, GR, and SLP display less pronounced seasonal changes, but reveal subtle intra-annual patterns. These plots allow for visual comparison of the seasonal distributions, identification of skewness, variability, and extremes, and provide a comprehensive overview of the stochastic behavior of each variable throughout the year. This visualization is particularly useful for

 doi:10.20944/preprints202603.2372.v1

understanding seasonal dynamics, validating models, or detecting long-term shifts in climate-related variables.

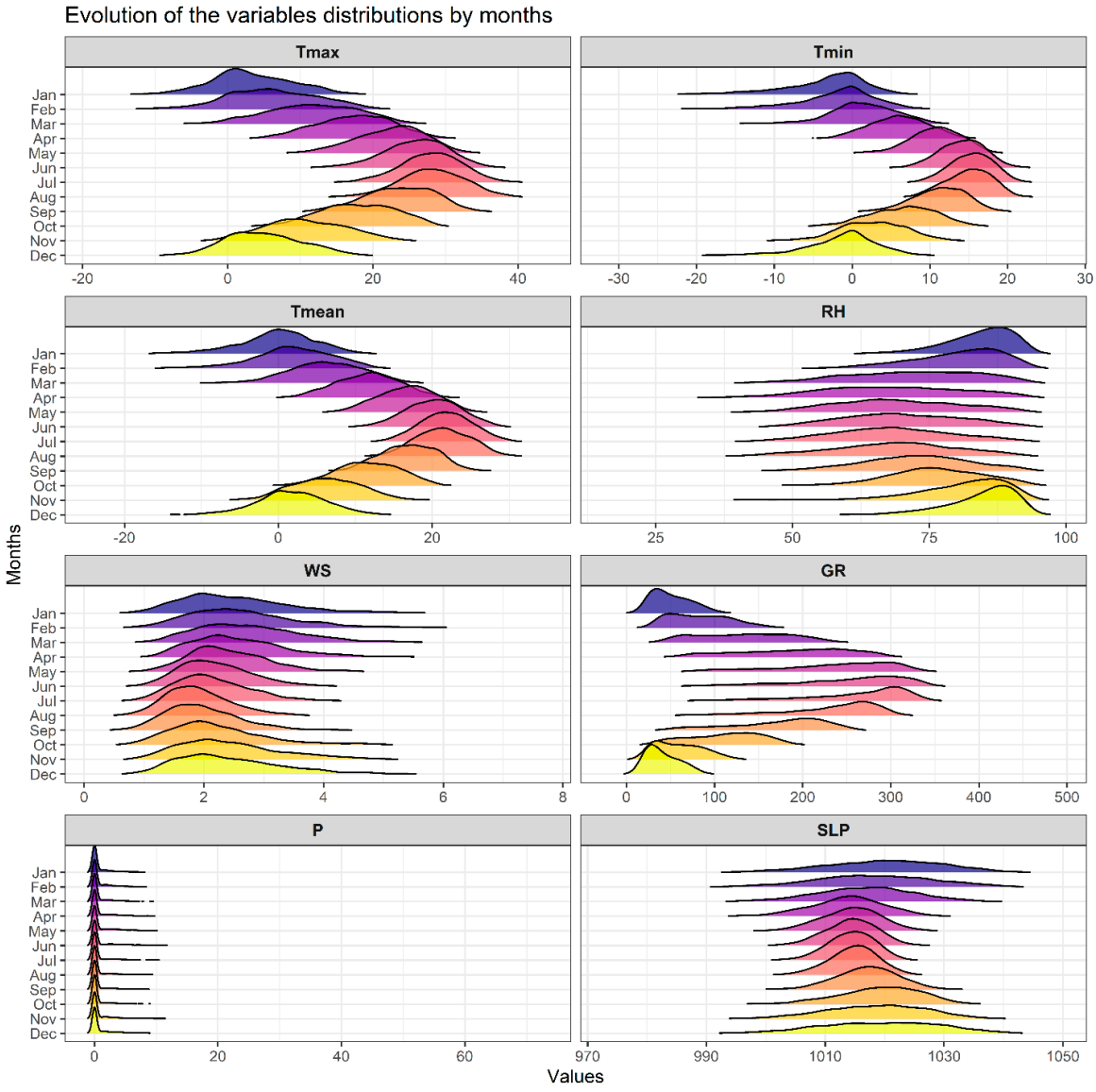

Figure 3. Seasonal distribution patterns of meteorological variables.

2.2. Estimation of Reference Evapotranspiration (ET_0)

The FAO Penman-Monteith method is widely recognized as the standard approach for calculating ET_0 based on meteorological data. It is recommended by the FAO [11]. This method combines energy balance and aerodynamic components, incorporating two resistance terms – surface and aerodynamic. Such a formulation provides highly accurate results, as it is grounded in physical principles and rational relationships [48]. In this study, the FAO-56 PM equation for estimating ET_0 is given by Allen et al. [11] as follows:

$$ET_0 = \frac{0.408\,\Delta\,(R_n - G) + \frac{900}{T+273}\,u_2(e_s - e_a)}{\Delta + \gamma(1 + 0.34u_2)} \quad (1)$$

Where ET_0 = reference evapotranspiration (mm day^{-1}), R_n = net radiation (MJ m^{-2} day^{-1}), G = soil heat flux density (MJ m^{-2} day^{-1}), T = mean daily air temperature at 2 m height (°C), u_2 = wind speed at 2 m height (m s^{-1}), e_s = saturation vapor pressure (kPa), e_a = actual vapor pressure (kPa), (e_s - e_a) =

 doi:10.20944/preprints202603.2372.v1

saturation vapor pressure deficit (kPa), Δ = slope of the vapor pressure curve (kPa °C^{-1}), and γ = psychrometric constant (kPa °C^{-1}).

2.3. Artificial Neural Networks (ANNs)

ANNs represent a form of nonlinear regression model that performs input-output mapping using a set of coefficients or weights [41,44]. ANNs are among the primary tools used in ML for pattern recognition, prediction, and forecasting [49], and have been successfully applied in various fields of scientific research. They consist of a network of processing units called neurons, which work collaboratively to solve specific problems. Typically, ANNs consist of input and output variables, along with one or more hidden layers (Figure 4). Each layer is fully connected to the subsequent layer through interconnection weights. These weights are initially assigned randomly and then adjusted during the training process [6]. The neural network layers contain multiple nodes and are structured as follows: (i) an input layer for introducing data into the system, (ii) one or more hidden layers for data processing during learning, and (iii) an output layer for generating predictions and decisions [50].

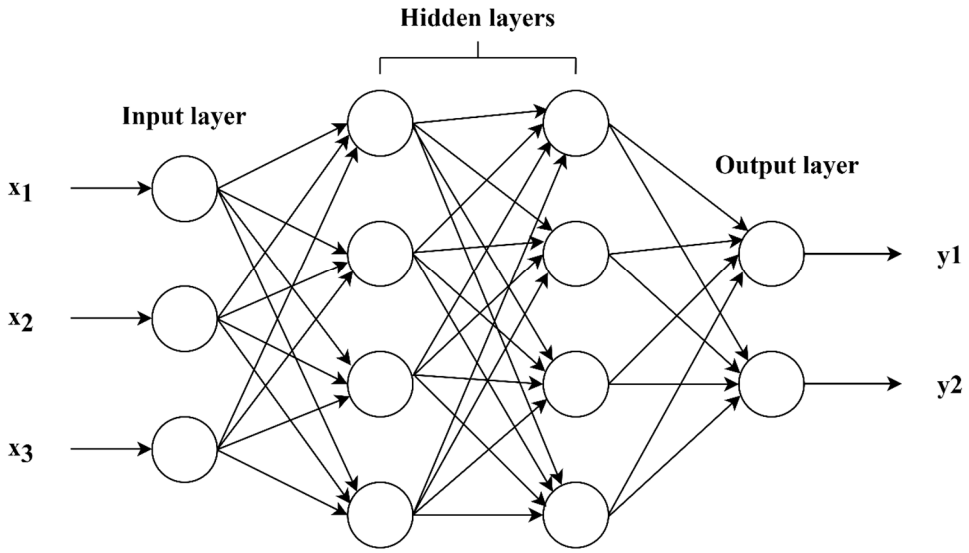

Figure 4. Architecture of the ANN model.

2.4. Performance Evaluation Criteria

The performance of the ANN models developed in this study was evaluated by comparing them with the reference FAO-56 PM method using standard statistical indicators, including the coefficient of determination (R^2), Nash-Sutcliffe efficiency (NSE), root mean square error (RMSE), and mean absolute error (MAE) (Table 2), to assess their accuracy and reliability.

Table 2. Model performance evaluation metrics.

No.	Performance Criteria	Equation	Acceptable Range
1	Coefficient of determination (R^2)	$R^2 = \frac{[\sum_{i=1}^{n}(X_i - \bar{X})(Y_i - \bar{Y})]^2}{\sum_{i=1}^{n}(X_i - \bar{X})^2 \sum_{i=1}^{n}(Y_i - \bar{Y})^2}$	0 to 1

 doi:10.20944/preprints202603.2372.v1

2	Nash-Sutcliffe efficiency (NSE)	$NSE = 1 - \frac{\sum_{i=1}^{n}(Y_i - X_i)^2}{\sum_{i=1}^{n}(X_i - \bar{X})^2}$	0 to 100
3	Root mean square error (RMSE)	$RMSE = \sqrt{\frac{1}{n}\sum_{i=1}^{n}(Y_i - X_i)^2}$	>0
4	Mean absolute error (MAE)	$MAE = \frac{1}{n}\sum_{i=1}^{n}\lvert Y_i - X_i \rvert$	>0

where n is the number of observations, X_i is the observed ET_0 value, Y_i is the estimated ET_0 value, $\bar{X}$ is the mean of the observed ET_0 values, and $\bar{Y}$ is the mean of the estimated ET_0 values.

3. Results and Discussion

3.1. FAO-56 PM Method

Daily ET_0 values were calculated for the period from 1950 to June 2023 using the FAO-56 PM method. Figure 5 illustrates the average daily ET_0 values over this period. ET_0 remained low during the winter months and progressively increased during spring, reaching its peak in July with a maximum of 8.4 mm day^{-1}. This seasonal trend is consistent with increased solar radiation, temperature, and wind speed during the summer.

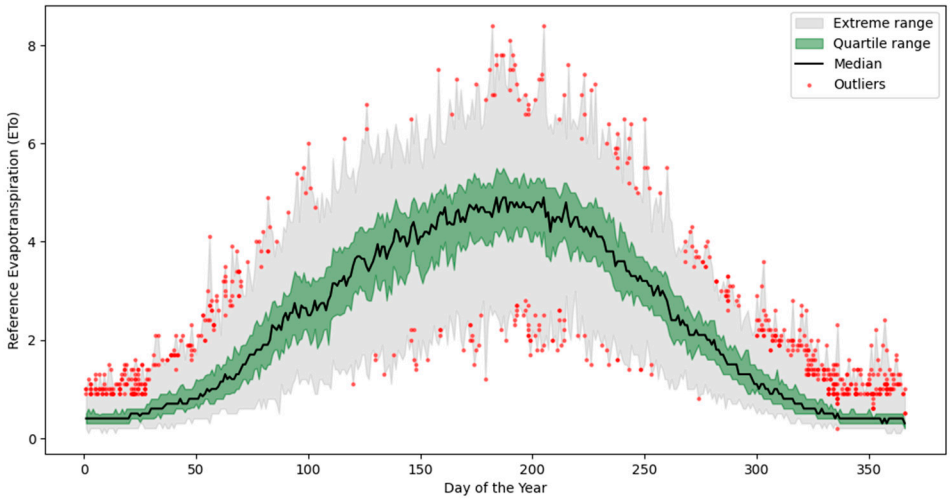

Figure 5. Multi-year average daily ET_0 at the Novi Sad station for the period 1950-2023.

The interquartile range indicates the spread of the middle 50% of the data, while the extreme range displays the minimum and maximum values recorded for each day. A higher number of outliers is observed during the summer months, likely resulting from interannual climatic variability and occasional extreme weather events.

These findings align with the expected seasonal dynamics of ET in temperate continental climates and underline the influence of meteorological factors such as temperature, radiation, and wind on daily ET_0 values.

3.2. Performance of ANN Models

The ANN model was developed using different combinations of input variables. For the period from 1950 to June 2023, the data were randomly divided into training, testing, and validation sets, with 70% of the data used for training, 20% for testing, and 10% for model validation.

 doi:10.20944/preprints202603.2372.v1

To examine the relationships between the meteorological variables used as model inputs, a pairwise scatterplot matrix (pairplot) was created (Figure 6). This visualization allows for the identification of potential linear and nonlinear dependencies between variables and provides an overview of their distributions. Strong linear correlation relationships are particularly evident among temperature-related parameters (T_{max}, T_{min}, T_{mean}), while other variables, such as WS, GR, P, and SLP, exhibit more scattered patterns.

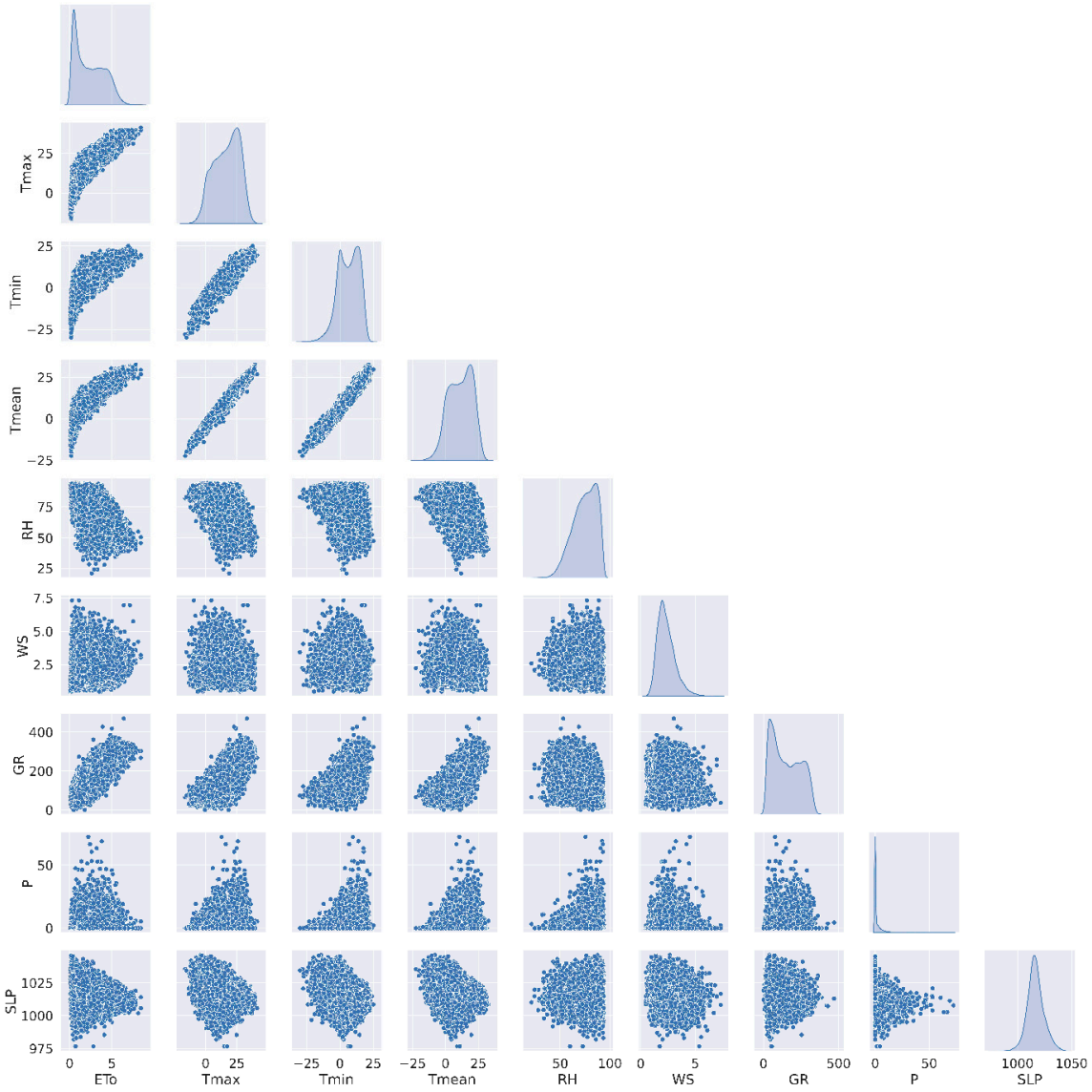

Figure 6. Pairplot of meteorological variables used as inputs for ET_0 modeling, showing scatter plots below the diagonal and variable distributions along the diagonal.

The model begins with an input layer in which all input variables are normalized to enhance learning efficiency. Normalization was performed to scale the input variables to a range between 0 and 1. The ANN model consists of hidden layers, each containing a specific number of neurons. The hyperbolic tangent (tanh) activation function was used in the hidden layers due to its ability to model nonlinear patterns in the data. The output layer consists of a single neuron that predicts the normalized ET_0 values, using a sigmoid activation to ensure that the output remains within the range of 0 to 1. For model training, the mean square error (MSE) was used as the loss function, while model optimization was performed using the Adam algorithm with default parameters and a learning rate of 1e-4. Additionally, L2 regularization was applied to each hidden layer with a regularization coefficient of 4e-5, whereas a reduced regularization value (1e-8) was applied to the final linear output

 doi:10.20944/preprints202603.2372.v1

layer. This approach contributes to improved model generalization. The training was conducted using a batch size of 1024, while validation results were evaluated every 10th or 50th epoch to accelerate the training process without compromising accuracy. This approach enabled faster model training while maintaining a high level of predictive performance and generalization.

The performance of the developed ANN models was evaluated based on different input combinations and compared with the FAO-56 PM reference method. As shown in Table 3, models with a greater number of input variables and more complex architectures consistently achieved better performance. The highest accuracy was obtained using all eight input parameters (T_{max}, T_{min}, T_{mean}, RH, WS, GR, P, SLP) with a two-hidden-layer architecture consisting of 32 and 16 neurons, respectively, resulting in R^2 = 0.98, NSE = 97.86%, RMSE = 0.25 mm day^{-1}, and MAE = 0.17 mm day^{-1}. This configuration demonstrated superior performance compared to other input combinations, indicating that the inclusion of the full set of parameters significantly enhances model precision.

Table 3. Performance of ANN models for the estimation of ET_0.

Input Combination	Hidden Neurons	FAO-56 PM			
		R^2	NSE	RMSE	MAE
T_{max}, T_{min}, T_{mean}, RH, WS, GR, P, SLP	32-16	0.98	97.86	0.25	0.17
T_{max}, T_{min}, T_{mean}, RH, WS, GR, P	16-8	0.98	97.70	0.26	0.18
T_{max}, T_{mean}, RH, WS, GR, P	16-8	0.98	97.58	0.27	0.19
T_{mean}, RH, WS, GR, P	10	0.97	97.08	0.29	0.21
T_{mean}, RH, WS, GR	12	0.97	96.78	0.31	0.22
T_{mean}, WS, GR	8	0.96	95.72	0.35	0.26
T_{mean}, GR	8-4	0.94	94.10	0.42	0.30
T_{mean}	4	0.86	86.43	0.63	0.49

The performance metrics in Table 3 illustrate a clear decline in model accuracy as the number of input variables decreases, emphasizing the importance of input diversity for ANN-based ET_0 estimation.

Slightly lower, yet still high, performance was achieved using the same inputs excluding SLP (R^2 = 0.98, NSE = 97.70%, RMSE = 0.26 mm day^{-1}, and MAE = 0.18 mm day^{-1}), as well as the configuration including T_{max}, Tmean, RH, WS, GR, P (R^2 = 0.98, NSE = 97.58%, RMSE = 0.27 mm day^{-1}, and MAE = 0.19 mm day^{-1}). The five-variable combination (T_{mean}, RH, WS, GR, P) with 10 neurons also showed strong performance, with R^2 = 0.97, NSE = 97.08%, RMSE = 0.29 mm day^{-1}, and MAE = 0.21 mm day^{-1}.

Among the models with a reduced number of inputs, the combination of T_{mean}, RH, WS, and GR also performed well with R^2 = 0.97, NSE = 96.78%, RMSE = 0.31 mm day^{-1}, and MAE = 0.22 mm day^{-1}, demonstrating that temperature and radiation-related parameters are key contributors to ET_0 prediction accuracy. Similarly, the model using only three inputs (T_{mean}, WS, GR) also performed well, with R^2 = 0.96, NSE = 95.72%, RMSE = 0.35 mm day^{-1}, and MAE = 0.26 mm day^{-1}. In the case of the two-input configuration, the best performance was observed for the composite of T_{mean} and GR using a two-hidden-layer architecture with 8 and 4 neurons, respectively. The model achieved R^2 = 0.94, NSE = 94.10%, RMSE = 0.42 mm day^{-1}, and MAE = 0.30 mm day^{-1}.

The configuration that included only T_{mean} as the input variable achieved the best performance among single-input models, with R^2 = 0.86, NSE = 86.43%, RMSE = 0.63 mm day^{-1}, and MAE = 0.49

 doi:10.20944/preprints202603.2372.v1

mm day^{-1}. Although it outperformed other single-variable configurations, its accuracy remained substantially lower than that of multi-input models. This outcome underscores the limitations of using a single meteorological parameter for estimating ET_0, as such models fail to capture the full complexity of ET dynamics. A gradual decline in performance was evident with the reduction in input dimensionality, as indicated by increasing RMSE and decreasing R^2 values.

The analysis indicates that ANN models are capable of generating highly accurate ET_0 estimates, especially when provided with a diverse set of meteorological inputs. Among the tested variables, T_{mean}, RH, WS, and GR were identified as the most influential, confirming previous findings in the literature.

These results are consistent with the findings reported by Makwana et al. [41], who demonstrated that ANN models with five input variables (T_{max}, T_{min}, RH, WS, BSS) outperformed simpler configurations and showed strong agreement with FAO-56 PM estimates. While their study identified Tmax as the most influential variable, the present analysis indicates that Tmean was the dominant factor for accurate ET_0 prediction. In this study, the model using only Tmean achieved R^2 = 0.86, NSE = 85.84%, RMSE = 0.64 mm day^{-1}, and MAE = 0.50 mm day^{-1}, while the model with only Tmax yielded nearly identical performance (R^2 = 0.86, NSE = 85.82%, RMSE = 0.64 mm day^{-1}, and MAE = 0.50 mm day^{-1}), indicating that both variables are similarly informative when used individually. Both studies confirm the effectiveness of ANN models in estimating ET_0 based on selected meteorological parameters.

4. Conclusions

This study evaluated the effectiveness of ANN models in estimating ET_0 using meteorological data from the Novi Sad station (Vojvodina, Serbia). Various input combinations and ANN architectures were tested and compared with the FAO-56 PM method. The results showed that ANN models can accurately predict ET_0, especially when a larger number of meteorological parameters is included. The highest performance was achieved using all eight input variables (T_{max}, T_{min}, T_{mean}, RH, WS, GR, P, SLP) with a two-hidden-layer structure, resulting in R^2 = 0.98, NSE = 97.86%, RMSE = 0.25 mm day^{-1}, and MAE = 0.17 mm day^{-1}. This result suggests that model accuracy improves with greater input diversity and proper network design. Models with reduced input sets also demonstrated satisfactory performance, particularly those including T_{mean}, WS, and GR, which were identified as the most influential for ET_0 prediction. The findings confirm the potential of ANN models as reliable tools for ET_0 estimation, indicating their suitability for application in regions with limited meteorological data availability. Future research could explore the application of other ML models, incorporate data from multiple meteorological stations, and include time series analysis to further improve ET_0 estimation accuracy.

Author Contributions: Conceptualization, M.S. and B.B.; methodology, B.B.; software, D.M.; validation, M.S. and D.M.; formal analysis, M.S.; investigation, M.S. and N.S.; data curation, N.S.; writing—original draft preparation, M.S.; writing—review and editing, R.S., A.B., A.S. and M.L.; supervision, B.B. and D.M. All authors have read and agreed to the published version of the manuscript.

Funding: This paper is funded by the Provincial Secretariat for Higher Education and Scientific Research of AP Vojvodina (Republic of Serbia), as part of the project entitled: Development of new water quality indices for Vojvodina in the context of sustainable agriculture and environmental protection (AQUA-QUAL) (contract no. 003876050 2025 09418 003 000 000 001 04 003).

Data Availability Statement: We encourage all authors of articles published in MDPI journals to share their research data. In this section, please provide details regarding where data supporting reported results can be found, including links to publicly archived datasets analyzed or generated during the study. Where no new data were created, or where data is unavailable due to privacy or ethical restrictions, a statement is still required. Suggested Data Availability Statements are available in section "MDPI Research Data Policies" at https://www.mdpi.com/ethics.

 doi:10.20944/preprints202603.2372.v1

Acknowledgments: This paper is supported by Ministry of Science, Technological Development and Innovation of the Republic of Serbia (451-03-137/2025-03/200117).

Conflicts of Interest: The authors declare no conflicts of interest.

References

1. Thomas, A. Development and Properties of 0.25-Degree Gridded Evapotranspiration Data Fields of China for Hydrological Studies. *Journal of Hydrology* **2008**, *358*, 145–158. https://doi.org/10.1016/j.jhydrol.2008.05.034
2. Komatsu, H.; Kume, T.; Otsuki, K. The Effect of Converting a Native Broad-Leaved Forest to a Coniferous Plantation Forest on Annual Water Yield: A Paired-Catchment Study in Northern Japan. *Forest Ecology and Management* **2008**, *255*, 880–886. https://doi.org/10.1016/j.foreco.2007.10.010
3. McVicar, T.R.; Roderick, M.L.; Donohue, R.J.; Li, L.T.; Van Niel, T.G.; Thomas, A.; Grieser, J.; Jhajharia, D.; Himri, Y.; Mahowald, N.M.; et al. Global Review and Synthesis of Trends in Observed Terrestrial Near-Surface Wind Speeds: Implications for Evaporation. *Journal of Hydrology* **2012**, *416–417*, 182–205. https://doi.org/10.1016/j.jhydrol.2011.10.024
4. Lin, P.; He, Z.; Du, J.; Chen, L.; Zhu, X.; Li, J. Impacts of Climate Change on Reference Evapotranspiration in the Qilian Mountains of China: Historical Trends and Projected Changes. *Intl Journal of Climatology* **2018**, *38*, 2980–2993. https://doi.org/10.1002/joc.5477
5. Saggi, M.K.; Jain, S. Reference Evapotranspiration Estimation and Modeling of the Punjab Northern India Using Deep Learning. *Computers and Electronics in Agriculture* **2019**, *156*, 387–398. https://doi.org/10.1016/j.compag.2018.11.031
6. Patil, A.P.; Deka, P.C. An Extreme Learning Machine Approach for Modeling Evapotranspiration Using Extrinsic Inputs. *Computers and Electronics in Agriculture* **2016**, *121*, 385–392. https://doi.org/10.1016/j.compag.2016.01.016
7. Kumar, M.; Raghuwanshi, N.S.; Singh, R.; Wallender, W.W.; Pruitt, W.O. Estimating Evapotranspiration Using Artificial Neural Network. *J. Irrig. Drain Eng.* **2002**, *128*, 224–233. https://doi.org/10.1061/(ASCE)0733-9437(2002)128:4(224)
8. Jahanbani, H.; El-Shafie, A.H. Application of Artificial Neural Network in Estimating Monthly Time Series Reference Evapotranspiration with Minimum and Maximum Temperatures. *Paddy Water Environ* **2011**, *9*, 207–220. https://doi.org/10.1007/s10333-010-0219-1
9. Abdullahi, J.; Elkiran, G. Prediction of the Future Impact of Climate Change on Reference Evapotranspiration in Cyprus Using Artificial Neural Network. *Procedia Computer Science* **2017**, *120*, 276–283. https://doi.org/10.1016/j.procs.2017.11.239
10. Trajkovic, S.; Kolakovic, S. Evaluation of Reference Evapotranspiration Equations under Humid Conditions. *Water Resour Manage* **2009**, *23*, 3057–3067. https://doi.org/10.1007/s11269-009-9423-4
11. Allen, R.G.; Pereira, L.S.; Raes, D.; Smith, M. Crop *Evapotranspiration: Guidelines for Computing Crop Water Requirements*; FAO Irrigation and Drainage Paper No. 56; Food and Agriculture Organization (FAO): Rome, Italy, 1998.
12. Fisher, D.K.; Pringle Iii, H.C. Evaluation of Alternative Methods for Estimating Reference Evapotranspiration. *AS* **2013**, *04*, 51–60. https://doi.org/10.4236/as.2013.48A008
13. Milly, P.C.D.; Dunne, K.A. Potential Evapotranspiration and Continental Drying. *Nature Clim Change* **2016**, *6*, 946–949. https://doi.org/10.1038/nclimate3046
14. Zhu, B.; Feng, Y.; Gong, D.; Jiang, S.; Zhao, L.; Cui, N. Hybrid Particle Swarm Optimization with Extreme Learning Machine for Daily Reference Evapotranspiration Prediction from Limited Climatic Data. *Computers and Electronics in Agriculture* **2020**, *173*, 105430. https://doi.org/10.1016/j.compag.2020.105430
15. Chia, M.Y.; Huang, Y.F.; Koo, C.H. Support Vector Machine Enhanced Empirical Reference Evapotranspiration Estimation with Limited Meteorological Parameters. *Computers and Electronics in Agriculture* **2020**, *175*, 105577. https://doi.org/10.1016/j.compag.2020.105577

 doi:10.20944/preprints202603.2372.v1

16. Basso, B.; Martinez-Feria, R.A.; Rill, L.; Ritchie, J.T. Contrasting Long-Term Temperature Trends Reveal Minor Changes in Projected Potential Evapotranspiration in the US Midwest. *Nat Commun* **2021**, *12*, 1476. https://doi.org/10.1038/s41467-021-21763-7
17. Tabari, H.; Grismer, M.E.; Trajkovic, S. Comparative Analysis of 31 Reference Evapotranspiration Methods under Humid Conditions. *Irrig Sci* **2013**, *31*, 107–117. https://doi.org/10.1007/s00271-011-0295-z
18. Kisi, O.; Sanikhani, H.; Zounemat-Kermani, M.; Niazi, F. Long-Term Monthly Evapotranspiration Modeling by Several Data-Driven Methods without Climatic Data. *Computers and Electronics in Agriculture* **2015**, *115*, 66–77. https://doi.org/10.1016/j.compag.2015.04.015.
19. Zhang, D.; Lin, J.; Peng, Q.; Wang, D.; Yang, T.; Sorooshian, S.; Liu, X.; Zhuang, J. Modeling and Simulating of Reservoir Operation Using the Artificial Neural Network, Support Vector Regression, Deep Learning Algorithm. *Journal of Hydrology* **2018**, *565*, 720–736. https://doi.org/10.1016/j.jhydrol.2018.08.050
20. Shu, Z.; Zhou, Y.; Zhang, J.; Jin, J.; Wang, L.; Cui, N.; Wang, G.; Zhang, J.; Wu, H.; Wu, Z.; et al. Parameter Regionalization Based on Machine Learning Optimizes the Estimation of Reference Evapotranspiration in Data Deficient Area. *Science of The Total Environment* **2022**, *844*, 157034. https://doi.org/10.1016/j.scitotenv.2022.157034
21. Monteith, J.L. Evaporation and environment. In *The State and Movement of Water in Living Organisms*; Proceedings of the 19th Symposium of the Society for Experimental Biology; Cambridge University Press: Cambridge, UK, 1965; pp. 205–234.
22. Droogers, P.; Allen, R.G. Estimating Reference Evapotranspiration under Inaccurate Data Conditions. *Irrigation and Drainage Systems* **2002**, *16*, 33–45. https://doi.org/10.1023/A:1015508322413
23. Trajkovic, S. Hargreaves versus Penman-Monteith under Humid Conditions. *J. Irrig. Drain Eng.* **2007**, *133*, 38–42. https://doi.org/10.1061/(ASCE)0733-9437(2007)133:1(38)
24. Traore, S.; Wang, Y.-M.; Kerh, T. Artificial Neural Network for Modeling Reference Evapotranspiration Complex Process in Sudano-Sahelian Zone. *Agricultural Water Management* **2010**, *97*, 707–714. https://doi.org/10.1016/j.agwat.2010.01.002
25. Almorox, J.; Quej, V.H.; Martí, P. Global Performance Ranking of Temperature-Based Approaches for Evapotranspiration Estimation Considering Köppen Climate Classes. *Journal of Hydrology* **2015**, *528*, 514–522. https://doi.org/10.1016/j.jhydrol.2015.06.057
26. Feng, Y.; Cui, N.; Zhao, L.; Hu, X.; Gong, D. Comparison of ELM, GANN, WNN and Empirical Models for Estimating Reference Evapotranspiration in Humid Region of Southwest China. *Journal of Hydrology* **2016**, *536*, 376–383. https://doi.org/10.1016/j.jhydrol.2016.02.053
27. Jayashree, T.R.; Reddy, N.V.S.; Acharya, U.D.; Eslamian, S. Prediction of Reference Crop Evapotranspiration: Empirical and Machine Learning Approaches. In *Handbook of Hydroinformatics*; Elsevier, 2023; pp. 253–268 ISBN 9780128219614
28. Rahimi Khoob, A. Comparative Study of Hargreaves's and Artificial Neural Network's Methodologies in Estimating Reference Evapotranspiration in a Semiarid Environment. *Irrig Sci* **2008**, *26*, 253–259. https://doi.org/10.1007/s00271-007-0090-z
29. Dai, X.; Shi, H.; Li, Y.; Ouyang, Z.; Huo, Z. Artificial Neural Network Models for Estimating Regional Reference Evapotranspiration Based on Climate Factors. *Hydrological Processes* **2009**, *23*, 442–450. https://doi.org/10.1002/hyp.7153
30. Kumar, M.; Raghuwanshi, N.S.; Singh, R. Artificial Neural Networks Approach in Evapotranspiration Modeling: A Review. *Irrig Sci* **2011**, *29*, 11–25. https://doi.org/10.1007/s00271-010-0230-8
31. Martí, P.; Royuela, A.; Manzano, J.; Palau-Salvador, G. Generalization of Eto Ann Models through Data Supplanting. *J. Irrig. Drain Eng.* **2010**, *136*, 161–174. https://doi.org/10.1061/(ASCE)IR.1943-4774.0000152
32. Pour-Ali Baba, A.; Shiri, J.; Kisi, O.; Fard, A.F.; Kim, S.; Amini, R. Estimating Daily Reference Evapotranspiration Using Available and Estimated Climatic Data by Adaptive Neuro-Fuzzy Inference System (Anfis) and Artificial Neural Network (Ann). *Hydrology Research* **2013**, *44*, 131–146. https://doi.org/10.2166/nh.2012.074
33. Antonopoulos, V.Z.; Antonopoulos, A.V. Daily Reference Evapotranspiration Estimates by Artificial Neural Networks Technique and Empirical Equations Using Limited Input Climate Variables. *Computers and Electronics in Agriculture* **2017**, *132*, 86–96. https://doi.org/10.1016/j.compag.2016.11.011

 doi:10.20944/preprints202603.2372.v1

34. Ferreira, L.B.; Da Cunha, F.F.; De Oliveira, R.A.; Fernandes Filho, E.I. Estimation of Reference Evapotranspiration in Brazil with Limited Meteorological Data Using ANN and SVM – A New Approach. *Journal of Hydrology* **2019**, *572*, 556–570. https://doi.org/10.1016/j.jhydrol.2019.03.028
35. Jyothi; G. V. Srinivasa Reddy; B. Maheshwara Babu; Prasad S. Kulkarni; Ananda N Artificial Neural Network Models for Estimation of Potential Evapotranspiration in a Semi-Arid Region of Raichur, Karnataka. *JAEI* **2020**, *57*, 172–181. https://doi.org/10.52151/jae2020572.1713
36. Kisi, O. Generalized Regression Neural Networks for Evapotranspiration Modelling. *Hydrological Sciences Journal* **2006**, *51*, 1092–1105. https://doi.org/10.1623/hysj.51.6.1092
37. Landeras, G.; Ortiz-Barredo, A.; López, J.J. Comparison of Artificial Neural Network Models and Empirical and Semi-Empirical Equations for Daily Reference Evapotranspiration Estimation in the Basque Country (Northern Spain). *Agricultural Water Management* **2008**, *95*, 553–565. https://doi.org/10.1016/j.agwat.2007.12.011
38. Walczak, S.; Cerpa, N. Artificial Neural Networks. In *Encyclopedia of Physical Science and Technology*; Elsevier, 2003; pp. 631–645 ISBN 9780122274107
39. Mallikarjuna, P.; Jyothy, S.A.; Sekhar Reddy, K.C. Daily Reference Evapotranspiration Estimation Using Linear Regression and Ann Models. *J. Inst. Eng. India Ser. A* **2012**, *93*, 215–221. https://doi.org/10.1007/s40030-013-0030-2
40. Dimitriadou, S.; Nikolakopoulos, K.G. Artificial Neural Networks for the Prediction of the Reference Evapotranspiration of the Peloponnese Peninsula, Greece. *Water* **2022**, *14*, 2027. https://doi.org/10.3390/w14132027
41. Makwana, J.J.; Deora, B.S.; Parmar B.S.; Patel, C.K.; Saini, A.K. Modelling of Reference Evapotranspiration Using Artificial Neural Network in Semi-Arid Region of North Gujarat. *JAEI* **2022**, *59*, 193–200. https://doi.org/10.52151/jae2022592.1775
42. Naresh, R.; Kumar, M.; Kumar, S.; Singh, K.; Sharma, P. Estimation of Reference Evapotranspiration Using Artificial Neural Network Models for Semi-Arid Region of Haryana. *J. Agrometeorol.* **2023**, *25*. https://doi.org/10.54386/jam.v25i1.1914
43. El-Magd, A.A.; Baraka, S.M.; Eid, S.F.M. Using artificial neural networks to predict the reference evapotranspiration. *Journal of Water and Land Development* **2023**, 1–8. https://doi.org/10.24425/jwld.2023.143768
44. Makwana, J.J.; Tiwari, M.K.; Deora, B.S. Development and Comparison of Artificial Intelligence Models for Estimating Daily Reference Evapotranspiration from Limited Input Variables. *Smart Agricultural Technology* **2023**, *3*, 100115. https://doi.org/10.1016/j.atech.2022.100115
45. Kumar, S.; Sharda, R.; Goyal, P.; Siag, M.; Kaur, P. Reference Evapotranspiration Modelling Using Artificial Neural Networks under Scenarios of Limited Weather Data: A Case Study in the Malwa Region of Punjab. *Environ Model Assess* **2024**, *29*, 589–620. https://doi.org/10.1007/s10666-023-09930-0
46. Skhiri, A.; Ferhi, A.; Bousselmi, A.; Khlifi, S.; Mattar, M.A. Artificial Neural Network for Forecasting Reference Evapotranspiration in Semi-Arid Bioclimatic Regions. *Water* **2024**, *16*, 602. https://doi.org/10.3390/w16040602
47. Copernicus Climate Change Service (C3S). Climate Data and Services. Implemented by ECMWF as part of the Copernicus Programme. Available online: https://climate.copernicus.eu (accessed on 6 February 2024).
48. Jensen, M.E.; Burman, R.D.; Allen, R.G., Eds. *Evapotranspiration and Irrigation Water Requirements*; American Society of Civil Engineers (ASCE): New York, USA, 1990.
49. Maier, H.R.; Dandy, G.C. Neural Networks for the Prediction and Forecasting of Water Resources Variables: A Review of Modelling Issues and Applications. *Environmental Modelling & Software* **2000**, *15*, 101–124. https://doi.org/10.1016/S1364-8152(99)00007-9
50. Liakos, K.; Busato, P.; Moshou, D.; Pearson, S.; Bochtis, D. Machine Learning in Agriculture: A Review. *Sensors* **2018**, *18*, 2674. https://doi.org/10.3390/s18082674